JOURNAL OF MATERIALS SCIENCE 35 (2000) 4653–4659

Determination of bond strength in glass fibre reinforced cement using petrography and image analysis

P. PURNELL*, A. J. BUCHANAN, N. R. SHORT, C. L. PAGE, A. J. MAJUMDAR
School of Engineering & Applied Science, Aston University, Birmingham, B4 7ET, UK
E-mail: pp@eng.warwick.ac.uk

The reinforcement in glass fibre reinforced cement (grc) is not present as discrete fibres, but as 'strands' of about 200 filaments each. This configuration greatly complicates determination of the 'perimeter' of the reinforcing elements, a crucial parameter in bond strength determination. Previous investigators have attempted to quantify strand perimeters but their methods have always involved at least one subjective step and are prone to operator bias. This paper describes an objective method of determining strand perimeters using digital analysis of images captured from petrological thin sections. The measured perimeters were found to be sensitive to the "threshold value" chosen for the analysis, and consideration of perimeter vs. threshold value curves eliminated subjectivity involved in the analysis. The perimeter value obtained, together with microscopic analysis of the crack patterns produced during tensile testing, were used for calculating bond parameters for different cement matrices. The development of bond with both ageing time and temperature were also studied. The method uses fundamental image analysis concepts and as such is readily adaptable to solve conceptually similar problems in a wide range of materials.

1. Introduction

The mechanical properties of commercial glass fibre reinforced cement (grc) are strongly dependent on the fibre-matrix bond. Evaluating this bond in traditional composites is difficult [1] and in the case of grc, assessment is further complicated by two factors. First, as the cement continues to hydrate the nature of the interface and hence magnitude of bond between fibre and matrix is likely to change, with implications for long-term durability. Secondly, the unit reinforcement element in grc is not a single glass filament with a well defined perimeter, and hence contact area, but a strand of more than 200 individual filaments whose perimeter is difficult to define. Inspection of cross-sections of grc clearly shows that, at least at early ages, the matrix does not penetrate far into the strand and the contact perimeter between fibre and matrix is not the sum of the filament perimeters. Furthermore the cross-sectional morphology of these strands is highly varied.

Direct measurement of bond strength in grc has been attempted by many investigators, generally by means of pull-out tests, see e.g. [2–5] where a strand is pulled out of a collar of matrix and a load-displacement curve obtained. The analysis of these curves is not straightforward; results are heavily dependent on embedded length and often exhibit large scatter owing to unstable debonding effects. To avoid calculating the strand perimeter, results are generally presented in terms of 'shear flow' [2], which is defined as the product of bond strength τ, and the strand perimeter P_f. More refined tests using a micro-indentation apparatus [6, 7] have not yet produced quantitative results.

Indirect measurement of bond strength in continuous, unidirectionally-reinforced, brittle-matrix composites can be effected using Aveston-Cooper-Kelly (ACK) theory [8–10]. This relates the spacing X, between the parallel transverse cracks formed during tensile testing of such composites to the frictional shear stress transfer rate, i.e. frictional bond τ, between the fibre and the matrix as given by Equation 1:

$$\tau = 1.364\left(\frac{V_m}{V_f}\right)\left(\frac{\sigma_{mu}}{X}\right)\left(\frac{A_f}{P_f}\right) \quad (1)$$

where V_m and V_f are the matrix and fibre volume fraction respectively, σ_{mu} is the matrix strength and A_f and P_f the cross-sectional area and perimeter of the reinforcing strands respectively. Examples of using this approach are given in references [11] and [12]. Although other models of the stress-strain behaviour of brittle matrix composites have been advanced, they require parameters which are very difficult to measure or derive for grc [5, 13] and often involve complex fracture mechanics [14] which can be difficult to apply in practical situations. The ACK model uses quantifiable

* Current affiliation: Division of Civil & Mechanical Engineering, University of Warwick, Coventry, UK, CV4 7AL.

parameters to model the stress-strain behaviour of grc and predict frictional bond values.

To derive frictional bond values (as opposed to shear flow values) a knowledge of P_f is required and investigators who have used the indirect method generally attempt to obtain it. Oakley and Proctor [11] examined sections of grc and deduced a perimeter of 2.83 mm for the 'standard' 204 filament strand although they did not give their method. This value has been used without comment by later authors [15, 4]. More recently, Kakemi *et al.* [12] traced the shapes of the glass fibre strands and analysed them using a Quantimet 920 image analyser. They deduced a perimeter of 1.097 mm (SD 0.143) for a 100-filament strand. Assuming that strand perimeter is approximately proportional to N^a (where $N =$ the number of filaments therein and $0.5 \leq a \leq 1$; a will be close to unity for a cross-sectional morphology with a high aspect ratio) this appears a broadly similar result to Oakley and Proctor's [11]. Kakemi *et al.* [12] also estimated that the glass occupied 66% of the strand cross-sectional area. Although this approach uses image analysis it still relies on a manual tracing and is hence subjective.

All of the above work has been concerned with portland cement matrix grc. Composites made with new matrices may have differing strand cross-sectional morphologies. In particular, sulpho-aluminate modified matrices are known to be expansive which may induce 'squeezing' of the fibre strands, causing them to adopt more compact initial morphologies than in traditional grc.

The objectives of the work to be described were to:

- Produce a fully objective method of determining strand perimeters and cross-sectional areas, using an image analysis technique.
- Determine whether the values of perimeter and area were affected by ageing time or matrix formulation.
- Determine the bond vs. time behaviour under various ageing conditions.

2. Materials and sample preparation

GRC boards, $500 \times 500 \times 6$ mm, were manufactured by a hand lay-up process to incorporate 1.5% V_f of continuous, unidirectional, alkali-resistant glass fibre. Three cementitious matrices were used, representative of those commonly employed in commercial products;

- Matrix O: a standard OPC,
- Matrix M: a mixture of OPC with 20% w/w metakaolin,
- Matrix C: a commercial blend of OPC, calcium sulpho-aluminate clinker and metakaolin.

The boards were cured for 28 days at 20°C, 95% RH. Tensile test coupons, 205×50 mm, were cut from the boards. Some coupons were immediately tested to provide control data. Others were aged underwater for periods up to 1 year at 20, 38 and 65°C prior to testing. Matrix strength was derived from the resultant stress-strain curves using in-house software. Crack spacings over a gauge length of 75 mm were measured using a travelling microscope at 100× magnification. Four traverses were made per sample and the average number of cracks, C, recorded. X was then calculated as $75/C$ mm.

Standard 30 μm petrographic thin sections were then prepared from selected coupons. Final grinding was performed using a non-aqueous medium to prevent further hydration of the sections. In order to investigate any possible effect of ageing on reinforcement cross-sectional morphology, samples were taken from unaged, control coupons and compared with those taken from coupons aged for 56 days underwater at 20°C. Preliminary results suggested this ageing regime promoted the development of a relatively large bond strength.

The thin sections were examined using a petrological microscope at 100× magnification. Cross-polarised light was used with a 530 nm shift plate inserted to allow the non-crystalline glass fibres to be strongly contrasted against the matrix. The microscope was equipped with a video camera and PC allowing the capture of 512×512 pixel, 16 million colour TIFF images.

3. Image analysis technique

A wide variation of glass strand cross-sectional morphologies was encountered, a 'lens' shape being the dominant feature, Fig. 1. In order to take these variations into account during analysis, the images of nine different strands were captured from each sample. Image analysis to derive the perimeter/area of each strand was performed on a UNIX workstation using the public-domain, open-system GRASS package developed by the U.S Army Construction Engineering Laboratory, and was carried out in the following stages:

(i) The as-captured image, Fig. 2a, is distorted in that this square image actually represents an area of 1.011×0.689 mm and so the image is first corrected to give the actual rectangular field of view as seen in Fig. 2b. During this correction it is also converted to 256-level greyscale and equalised; the brightest pixel is set to 255, the darkest to zero and the other pixels scaled in brightness accordingly. This procedure increases the contrast of the displayed image without changing the information contained within it. The fibres appear much brighter than the surrounding matrix.

(ii) A cursor, which indicates the brightness of the pixel beneath it, is run over the interfacial area and a threshold brightness value, T, chosen. Parts of the image brighter than T are assumed to represent fibre and those darker to represent matrix. A 'binary slice' is then performed on the image on the basis of T; it is re-plotted with each pixel assigned a value of either 1 (fibre) or 0 (matrix) depending on whether its original grey-scale value (0 to 255) was above or below T, to give an image as shown in Fig. 2c.

(iii) This latter image must now be 'clumped'. Unwanted artefacts in the original image, e.g. pores, microcracks and small crystals, may also have appeared brighter than T and hence been erroneously classed

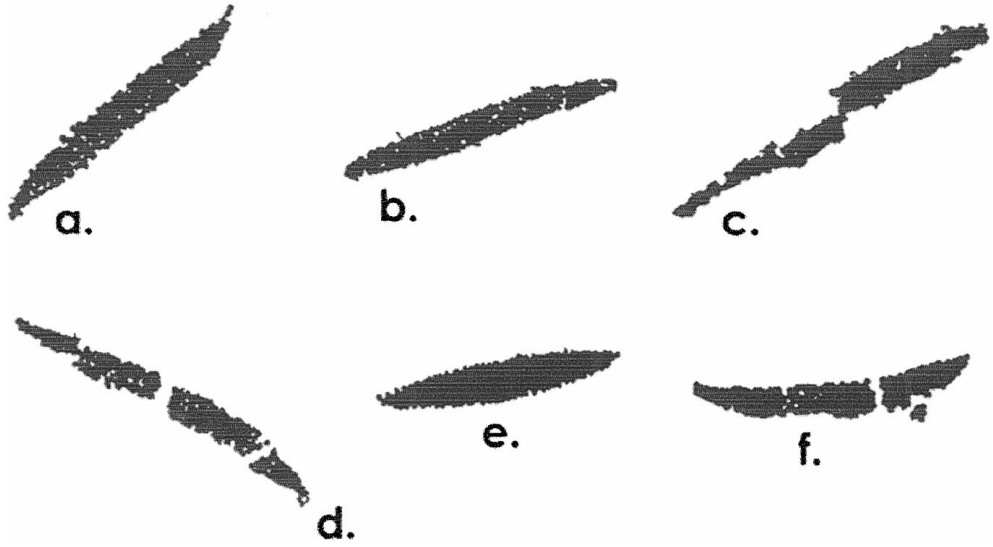

Figure 1 Typical strand cross-sectional morphologies.

as fibres. The image will have a large number (typically a few thousand) of small clumps of continuously adjoining 1-value pixels as well as the large clump representing the fibre strand. The program scans the image for these clumps and re-plots it, assigning each clump a unique colour value, Fig. 2d. A further binary slice is then performed on the image with the unique colour value of the fibre clump used as the threshold value. This removes all extraneous pixels, Fig. 2e.

(iv) The image now consists of a single clump of pixels. A small algorithm is then used to isolate the pixels forming the perimeter, and the image is finally plotted with just these pixels displayed, Fig. 2f. The perimeter can then be determined by either using vectorisation or the 'random walk' hypothesis. Vectorisation involves the GRASS system's vector image capabilities drawing a line through the centre of all the pixels and measuring its length. The random walk hypothesis (RWH) see Appendix, assumes that the length of the perimeter is proportional to the number of pixels therein. The perimeter algorithm also evaluates the area bounded within the perimeter; this allows the proportion of the strand not occupied by glass (i.e. the interfilamental area) to be deduced.

(v) It is important to note that occasionally the strand may be represented by more than one clump e.g. Fig. 1d and f, in which case the stages shown in Fig. 2d and e must be repeated for each clump.

The perimeter measurement process as described in stages (i)–(v) does not in itself represent an improvement on existing methods, as it still contains one subjective step. Since the fibre-matrix boundary is not unambiguously defined, a judgement of the best initial threshold value to be used in the analysis must be made. In order to investigate whether this subjectivity could be removed, the effect of varying the threshold value on the number of perimeter pixels extracted (which is closely proportional to the perimeter) was evaluated.

It was found that for all samples the number of perimeter pixels passed through a minimum, Fig. 3, at some optimum threshold value T_0. This value was always close to that chosen by visual means in the initial analysis. It was also found that T_0 was unique to each image i.e. a single threshold value could not be applied across a number of images despite their being taken from the same composite under the same lighting conditions etc.

The main justification for using the minimum perimeter/T_0 rationale is that T_0 is always close to the value intuitively chosen and that it can be objectively applied across all samples. It can be further justified by considering the changing shape of the fibre clump as the chosen threshold is varied. When $T < T_0$, the operation is being less selective about what is included; the fibre clump and hence the measured perimeter will be larger. Extraneous, non-fibre pixels may also be included further inflating the perimeter. As the limit $T \rightarrow 0$ is approached, nearly all the pixels in the image will be classed as fibre and the measured perimeter increases rapidly.

When $T > T_0$ the operation is being more selective. Fewer pixels will be included, but the coastline of the fibre clump will become more convoluted thus increasing its perimeter. This coastline will become increasingly unlikely to model the contact perimeter between fibre and matrix accurately. Groups of fibre pixels will separate from the main clump and care must be taken not to exclude these from the analysis. In the limit, the measured perimeter will approach the sum of the perimeters of the individual filaments. T_0 therefore represents a balance point between exclusion of noise and ensuring a realistic perimeter morphology.

4. Results and discussion

4.1. Perimeters - Influence of matrix composition/ageing

The derivation of T_0 (and the corresponding perimeter) could be applied consistently to all samples, removing the subjectivity involved in choosing a threshold value. Using this approach, the average strand perimeter after curing but before ageing for each matrix was derived, Fig. 4 (un-hatched bars). No significant differences in perimeter between the three different matrix grcs were

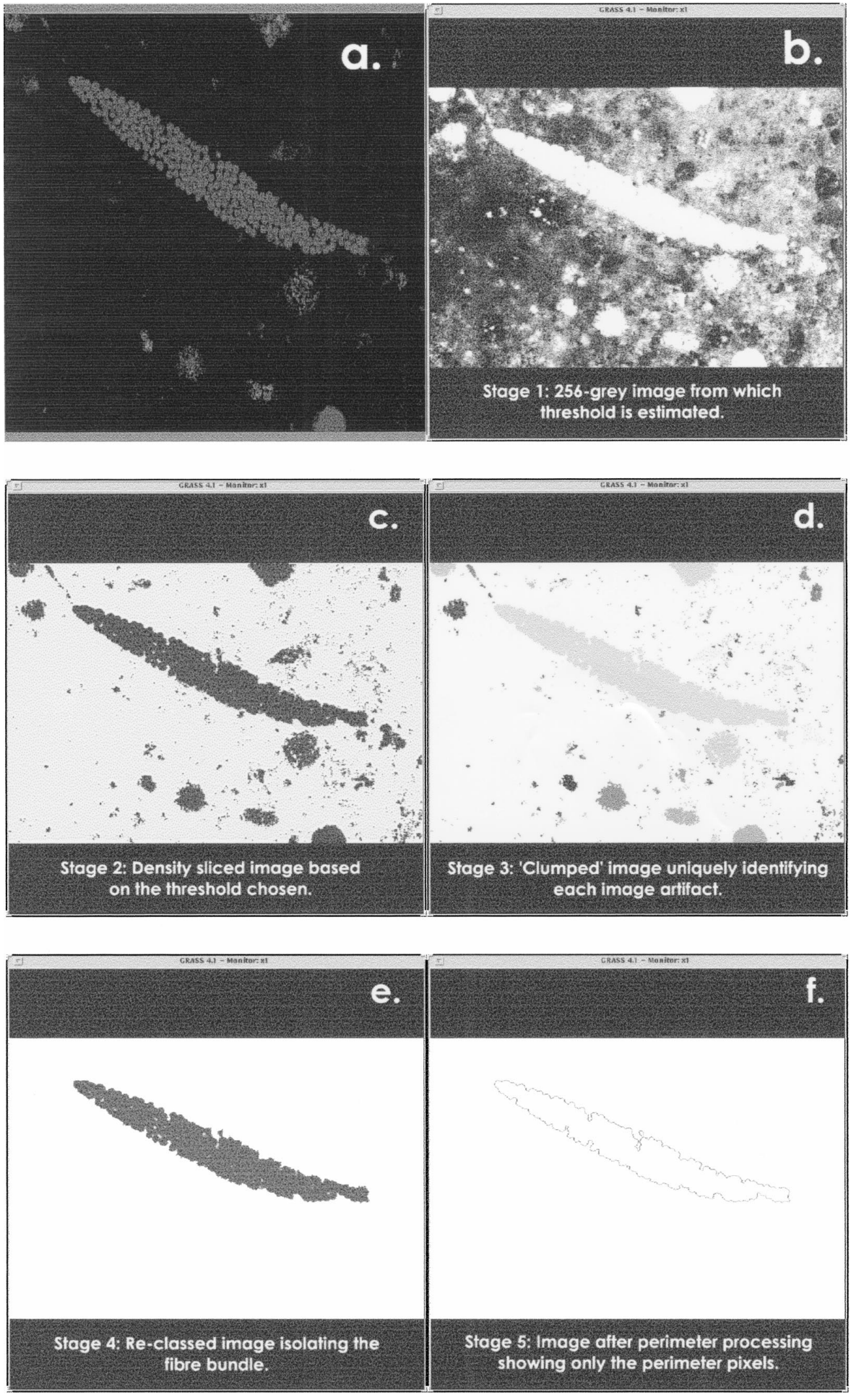

Figure 2 (a) Original image; (b) re-mapped grey image; (c) binary slice; (d) clumped image; (e) reclassed image; (f) isolated perimeter.

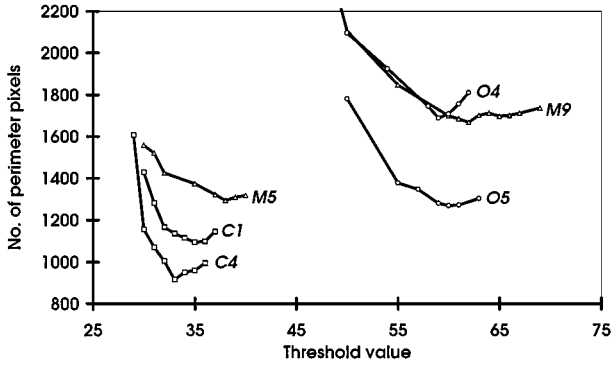

Figure 3 Number of perimeter pixels vs. threshold value.

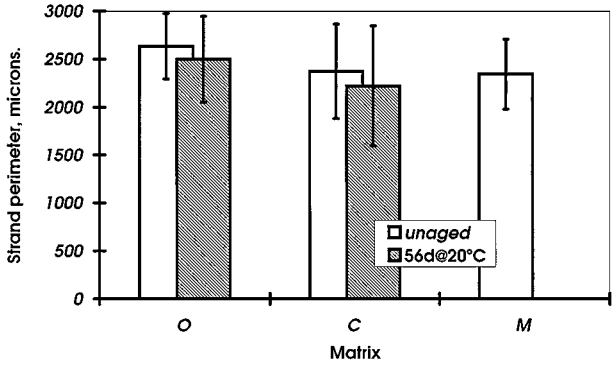

Figure 4 Strand perimeters. Error bars = ±1 standard deviation).

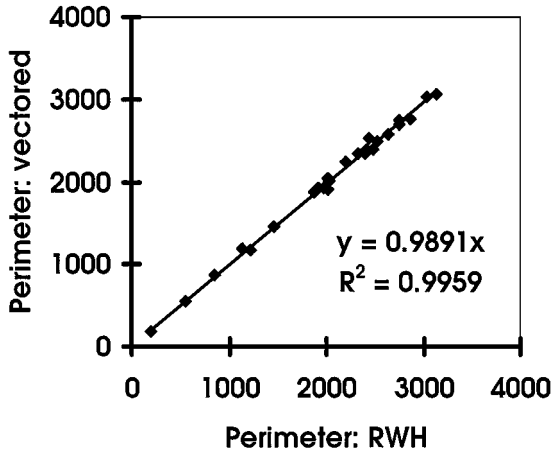

Figure 5 RWH vs. vector method (μm).

observed. For matrices O and C, strand perimeters after ageing were also derived, Fig. 4 (hatched bars). The ageing appeared to have no significant effect on the strand perimeters. The global mean perimeter (the mean of all measured perimeters) was found to be 2.404 mm with a standard deviation of 0.467 mm. This is about 15% lower than that derived by Oakley and Proctor [11].

In preliminary studies, both RWH and vectorisation were used in the final stage of perimeter determination. Results obtained (both from full, e.g. Fig. 1a, and partial, e.g. Fig. 1d, strands) using either method did not differ significantly, Fig. 5. RWH was used in the final study as it is the simpler procedure.

4.2. Interfilamental areas

The 'interfilamental area' (i.e. the area within the strand that was initially void space, A_I) was deduced by subtracting the constant cross-sectional area of glass in a strand (0.030 mm^2) from the area bounded by the measured perimeter. The results are shown in Fig. 6, where it can be seen that the mean A_I for unaged matrix O and M composites is not significantly different, 0.0179 and 0.0161 mm^2 respectively. In unaged matrix C composites, A_I is about 25% lower, 0.0125 mm^2. Analysis of variance confirms this as a significant result at the 95% level. Ageing, however, had no significant effect on A_I as shown for matrices O and C, Fig. 6 (hatched bars).

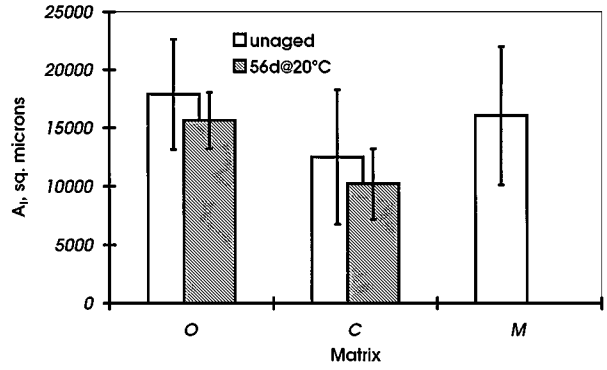

Figure 6 Strand inter-filamental areas. Error bars = ±1 standard deviation.

4.3. Frictional bond

Since neither matrix formulation or ageing had a significant effect on the strand perimeter, the global value, 2.40 mm, was used in Equation 1 to derive the frictional bond for all samples.

Fig. 7 shows bond vs. time curves for grc samples aged at 20°C. It may be seen that the frictional bond initially rises with ageing time, reaching a terminal value between 28 and 56 days i.e. after such time there is no statistically significant change in the frictional bond. Matrix C composites develop a significantly higher terminal bond than matrix O and M composites. It was

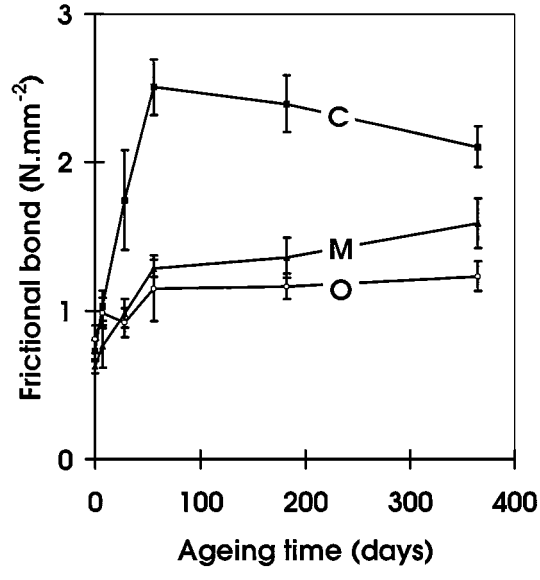

Figure 7 Frictional bond vs. ageing time @ 20°C. Error bars = ±1 standard error.

also found that the value of terminal bond attained was dependent on the ageing temperature, Fig. 8. Ageing at higher temperatures produced lower terminal bond values. It did not, however, appear to affect the rate of bond development, as is clearly shown for matrix C composites in Fig. 9.

The lower A_I in matrix C composites may be a contributing factor to the development of higher bond in these composites. Compared to the other grcs, the filaments within the strands are more efficiently packed together and there may be little room available within the strand for further rearrangement of the filaments. Any growth of hydration products at the strand-matrix interface and hence reduction in the space available to the strand would be less able to be taken up by further packing of the filaments. This may result in a 'pinching' force being applied to the strand in matrix C composites, thus increasing frictional bond.

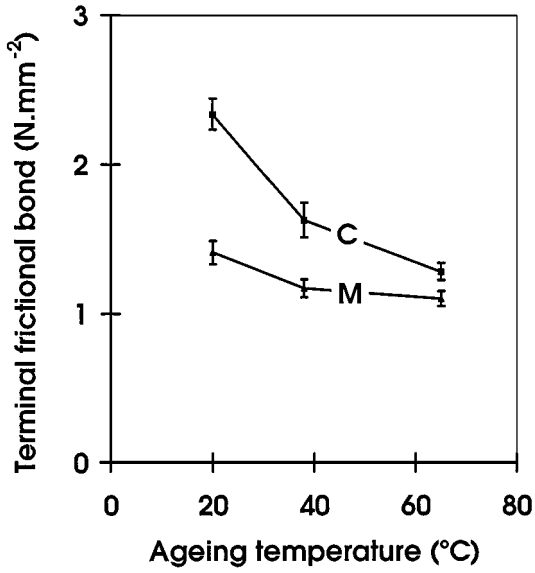

Figure 8 Terminal frictional bond vs. ageing temperature. Error bars = ±1 standard error.

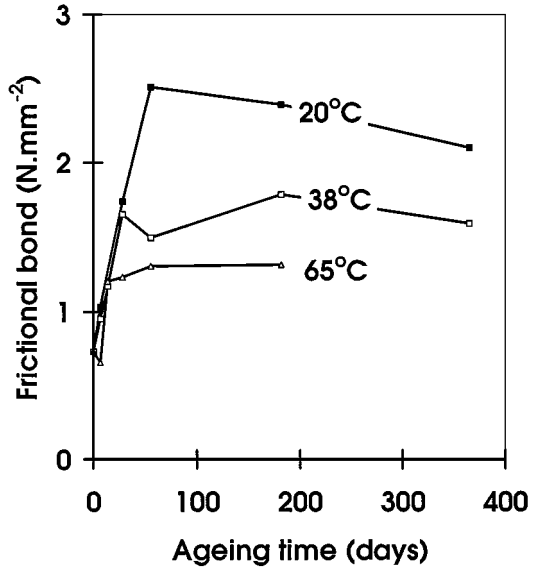

Figure 9 Frictional bond vs. ageing time & temperature; Matrix C.

The inverse relationship between ageing temperature and terminal frictional bond was unexpected. The reasons behind it are unclear, although it is known that different hydration products are formed in matrices M and C at higher temperatures [16, 17]. This finding may have implications for short fibre composites designed to exhibit pseudo-toughness via low-bond, fibre pull-out mechanisms. Since the bond formed at elevated temperatures, Fig. 8, is rather less than that formed at in-service temperatures, the hot water accelerated ageing regime may give false grounds for confidence with regards to long-term retention of toughness.

5. Conclusions

An objective method of determining strand perimeters in grc composites has been developed using digital analysis of images captured from petrological thin sections. This should make comparison of results from different investigations easier.

The perimeter of *in-situ* AR-glass fibre strands does not vary significantly between matrices or with ageing time. A constant mean perimeter of 2.40 mm can be used in all calculations. However, the analysis does suggest that with calcium-sulphoaluminate modified matrices the filaments within a strand became more efficiently packed during initial setting, probably due to the expansive nature of the matrix.

Using the perimeter value derived, bond vs. time curves for grc with three different matrices have been produced. Frictional bond reached a terminal value between 28 and 56 days of ageing. Matrix C grc developed a significantly larger terminal frictional bond than the other grc composites studied. The value of terminal bond achieved is affected by accelerated ageing temperature; higher temperatures produced a lower terminal bond.

Appendix: Random walk hypothesis

Consider traversing a closed loop consisting of a string of N pixels each of width x and height y. If the loop is sufficiently long and convoluted that each of the 8 possible step paths, Fig. 10, (OA, OB. . .OH) from one pixel centre to the next is taken an equal number of times during the traverse then the length of the loop (i.e. the perimeter, P) is given by;

$$P = \frac{1}{4}N[x + y + 2\sqrt{(x^2 + y^2)}].$$

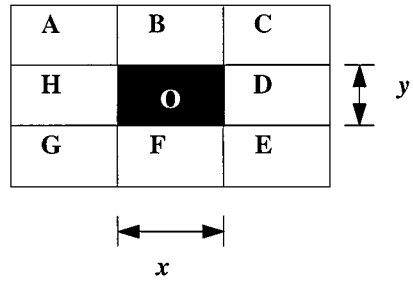

Figure 10 Possible pixel-pixel step paths.

Acknowledgements

Financial support from the Engineering and Physical Sciences Research Council (GR/K 05436) and materials from CemFIL International and Blue Circle are gratefully acknowledged.

References

1. D. TRIPATHI and F. R. JONES, *J. Mater. Sci.* **33** (1998) 1.
2. P. BARTOŠ, *ibid.* **15** (1980) 3122.
3. *Idem.*, in Proceedings of the PCI Symposium on Durability of Glassfiber Reinforced Concrete, Illinois, USA, November 1985, edited by S. Diamond, p. 136.
4. V. LAWS, A. A. LANGLEY and J. M. WEST, *J. Mater. Sci.* **21** (1986) 289.
5. E. A. NAAMAN, G. G. NAMUR, J. M. ALWAN, and H. S. NAJM, *J. Structural Eng.* **117** (1991) 2791.
6. W. ZHU and P. J. M. BARTOŠ, *Cem. Concr. Res.* **27** (1997) 1701.
7. P. J. M. BARTOŠ and W. ZHU, *Cem. Concr. Composites* **18** (1996) 31.
8. J. AVESTON, G. A. COOPER and A. KELLY, in Proceedings of the NPL Conference, UK, November 1971 (IPC Science and Technology Press 1971) p. 15.
9. J. AVESTON and A. KELLY, *J. Mater. Sci.* **8** (1973) 352.
10. J. AVESTON, R. A. MERCER and J. M. SILLWOOD, in Proceedings of the NPL Conference, UK, April 1974 (UK, IPC Science and Technology Press, 1974) p. 93.
11. D. R. OAKLEY and B. A. PROCTER, in Proceedings of the RILEM Symposium on Fibre Reinforced Cement and Concrete, London, September 1975, edited by A. Neville (UK, Lancs., Construction Press) p. 347.
12. M. KAMEKI, D. J. HANNANT and M. MULHERON, *Mag. Concr. Res.* **48** (1996) 229.
13. S. P. SHAH, in Proceedings of the PCI Symposium on Durability of Glassfiber Reinforced Concrete, Illinois, USA, November 1985, edited by S. Diamond, p. 91.
14. S. H. LI, Z. LI, T. MURA and S. P. SHAH, *Eng. Fracture Mechanics* **43** (1992) 561.
15. V. LAWS, *Composites* **113** (1982) 145.
16. P. PURNELL, PhD Thesis, Aston University, 1998.
17. P. PURNELL, N. R. SHORT, C. L. PAGE, A. J. MAJUMDAR and P. L. WALTON, *Composites Pt. A* **30** (1999) 1073.

Received 15 June 1999
and accepted 30 March 2000